Protein Science (2000), *9*:1857–1865. Cambridge University Press. Printed in the USA.

Successful molecular dynamics simulation of the zinc-bound farnesyltransferase using the cationic dummy atom approach

YUAN-PING PANG,[1,2,3,4] KUN XU,[2] JAMAL EL YAZAL,[3] AND FRANKLYN G. PRENDERGAST[1,2,3]

[1]Mayo Clinic Cancer Center, Mayo Foundation for Medical Education and Research, 200 First Street SW, Rochester, Minnesota 55905
[2]Tumor Biology Program, Mayo Foundation for Medical Education and Research, 200 First Street SW, Rochester, Minnesota 55905
[3]Department of Molecular Pharmacology and Experimental Therapeutics, Mayo Foundation for Medical Education and Research, 200 First Street SW, Rochester, Minnesota 55905
[4]Molecular Neuroscience Program, Mayo Foundation for Medical Education and Research, 200 First Street SW, Rochester, Minnesota 55905

(RECEIVED April 12, 2000; FINAL REVISION July 11, 2000; ACCEPTED July 14, 2000)

Abstract

Farnesyltransferase (FT) inhibitors can suppress tumor cell proliferation without substantially interfering with normal cell growth, thus holding promise for cancer treatment. A structure-based approach to the design of improved FT inhibitors relies on knowledge of the conformational flexibility of the zinc-containing active site of FT. Although several X-ray structures of FT have been reported, detailed information regarding the active site conformational flexibility of the enzyme is still not available. Molecular dynamics (MD) simulations of FT can offer the requisite information, but have not been applied due to a lack of effective methods for simulating the four-ligand coordination of zinc in proteins. Here, we report in detail the problems that occurred in the conventional MD simulations of the zinc-bound FT and a solution to these problems by employing a simple method that uses cationic dummy atoms to impose orientational requirement for zinc ligands. A successful 1.0 ns (1.0 fs time step) MD simulation of zinc-bound FT suggests that nine conserved residues (Asn127α, Gln162α, Asn165α, Gln195α, His248β, Lys294β, Leu295β, Lys353β, and Ser357β) in the active site of mammalian FT are relatively mobile. Some of these residues might be involved in the ligand-induced active site conformational rearrangement upon binding and deserve attention in screening and design of improved FT inhibitors for cancer chemotherapy.

Keywords: cancer research; coordination chemistry; drug research; farnesyltransferase; metalloproteins; molecular dynamics; zinc

Farnesyltransferase (FT) catalyzes the transfer of the farnesyl group from the co-substrate farnesyl pyrophosphate to a Cys residue in the C-terminal fragment of pro-Ras proteins. The resulting protein farnesylation is a key step in the post-translational modification of pro-Ras proteins (Park et al., 1997). This enzyme is a promising anticancer drug target (Gibbs & Oliff, 1997) as selective FT inhibitors (FTIs) are able to inhibit tumor cell proliferation without substantially interfering with normal cell growth (Kohl et al., 1993; Prendergast et al., 1994; Sebti & Hamilton, 1997). To develop improved FTIs through a structure-based drug design utilizing the crystal structure of FT (Park et al., 1997), the molecular flexibility of the enzyme active site needs to be determined in order to understand how ligands can be optimally accommodated.

Reprint requests to: Yuan-Ping Pang, Department of Pharmacology, Mayo Clinic Cancer Center, 200 First Street SW, Rochester, Minnesota 55905; e-mail: pang@mayo.edu.

Although several X-ray structures of free FT and inhibitor- and/or co-substrate-bound FT complexes have been reported (Park et al., 1997; Long et al., 1998, 2000; Strickland et al., 1998, 1999; Wu et al., 1999), detailed information about the active site conformational flexibility of the enzyme is still not available. Molecular dynamics (MD) simulations provide a logical strategy to obtain the required information on molecular flexibility and NMR spectroscopy, in principle, can yield direct data on protein dynamics. Unfortunately, the large molecular weight of FT, 94 kDa (Reiss et al., 1990), precludes the NMR approach and discourages MD simulations. Furthermore, a zinc divalent cation embedded in the active site of FT poses a technical complication in MD simulations. Two general methods have been reported for MD simulations of zinc proteins. One termed the "bonded model" (Hoops et al., 1991; Ryde, 1995; Lu & Voth, 1998) uses covalent bonds between the zinc ion and its coordinates to maintain zinc's four-ligand coordination in proteins during MD simulations. This method is not

suitable to the present study because the introduced covalent bonds rigidify the conformation of the active site. Although the rigidification problem can be avoided by use of an anharmonic potential such as a Morse oscillator (Lu & Voth, 1998), the anharmonic potential approach has not yet been adequately tested for its effectiveness in maintaining the four-ligand coordination of zinc in proteins. The second one, termed the "non-bonded model" (Vedani & Huhta, 1990; Aqvist & Warshel, 1992; Stote & Karplus, 1995; Wasserman & Hodge, 1996), maintains the four-ligand coordination of zinc in proteins with electrostatic and van der Waals forces to avoid the use of covalent bonds. The nonbonded model is, in principle, suitable to the MD simulation of FT, but it has been tested only in short (<100 ps) MD simulations. For these reasons, no MD simulations of FT have been reported. Recently, we have reported a simple method, termed the "cationic dummy atom model," which was successful in maintaining the four-ligand coordination of zinc without use of covalent bonds between zinc and its ligands in nanosecond-length MD simulations of three zinc proteins with which the MD simulations using the nonbonded model failed (Pang, 1999).

Here, we report in detail the problems that occurred in the MD simulations of the zinc-bound FT using the nonbonded model and a solution to these problems by employing the cationic dummy atom approach. We then present a successful 1.0 ns (1.0 fs time step) MD simulation of zinc-bound FT, which suggests that there are nine conserved residues in the active site of mammalian FT that are relatively mobile. Some of these residues might be involved in the ligand-induced active site conformational rearrangement upon binding and deserve attention in the screening and design of improved FT inhibitors for cancer chemotherapy.

Results

Deformation of the tetrahedral zinc complex

In an MD simulation of FT employing a neutral Cys299β as a zinc coordinate and a set of the reported force field parameters for the zinc divalent cation (r = 1.45 Å, ϵ = 0.025 kcal/mol) (Wasserman & Hodge, 1996), the zinc ion moved away from the position identified in the X-ray structure of FT, despite the fact that the zinc divalent cation was neutralized by two deprotonated, anionic coordinates of Asp297β and H_2O1002. A large basis set DFT calculation of the proton dissociation energy of zinc-coordinated methanethiol was thus performed (ElYazal & Pang, 1999) and confirmed the reported hypothesis that Cys residue would be deprotonated when coordinating to zinc in proteins (Ryde, 1996). Consequently, by using three anionic and one neutral coordinates (Cys^-299β, Asp^-297β, His362β, and HO^-1002) or by using two anionic and two neutral coordinates (Cys^-299β, Asp^-297β, His362β, and H_2O1002) in the MD simulation, the zinc ion was able to be kept in the desired position. However, a new problem arose: the four-ligand coordination of zinc (Zn^{2+}, Cys299β, His363β, Asp297β, and H_2O1002) was changed to a five ligand-coordination during the MD simulation. In the five-ligand complex, the zinc ion interacted with Asp352β that was initially away from the zinc ion but moved toward the zinc ion during the MD simulation (Fig. 1). Interestingly, in the FT structure with either two anionic coordinates (Cys^-299β and Asp^-297β) or three anionic coordinates (Cys^-299β, Asp^-297β, and HO^-1002), the four-ligand coordination of zinc was converted to a five-ligand coordination even after a 1,000-step energy minimization prior to the MD simulation. The four-ligand coordination could be retained in an energetically less stable protein structure if a 500-step energy minimization was performed. However, the four-ligand coordination was inevitably changed to the five-ligand coordination after a 2 ps MD simulation of the structure minimized with 500 steps; and the five-ligand coordination was maintained throughout a 200 ps MD simulation. Despite the fact that Asp352β was next to Lys353β forming a salt bridge in the crystal structure of FT, a simulation was also performed with deprotonated Asp352β replaced by a protonated Asp352β residue in the hope that the attractive electrostatic interaction arising from the negatively charged carboxylate group and the zinc cation could be reduced, thus preventing Asp352β from moving toward the zinc ion. Unfortunately, this attempt was proved fruitless.

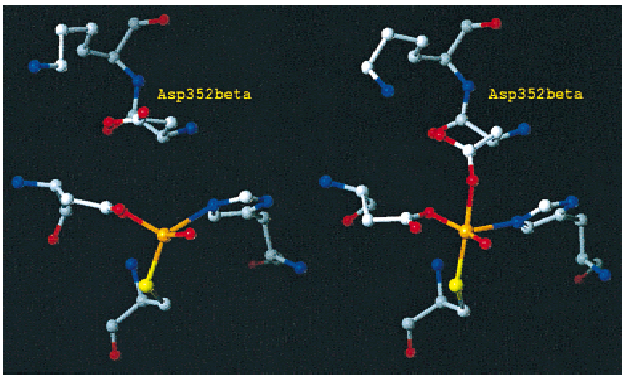

Fig. 1. Move of Asp352β toward the zinc cation resulting in a conversion of a tetrahedral zinc complex (left: crystal structure) to a trigonal bipyramidal complex (right: MD structure) during the MD simulations without use of the cationic dummy atom approach (Zn, orange; O, red; N, blue; and C, white).

The problem that the nearby Asp352β moved toward the zinc ion forming a five-coordinate zinc complex was akin to a reported problem in the MD simulation of carbonic anhydrase in which a nearby Glu106 moved toward the zinc ion (Hoops et al., 1991; Stote & Karplus, 1995). The problem in the simulation of carbonic anhydrase was solved by computing the long-range electrostatic interactions and by employing harmonic restraints on the zinc complex during the energy minimization that were then removed by a gradual reduction during the MD simulation (Stote & Karplus, 1995). The calculation of the long-range electrostatic interactions was reportedly crucial to avoiding having Glu106 move toward to the zinc ion during an 80 ps simulation of carbonic anhydrase employing the CHARMM force field (Stote & Karplus, 1995). Nevertheless, in the simulation of FT employing the AMBER 95 force field (Cornell et al., 1995), the five-ligand coordination occurred regardless whether the long-range electrostatic interactions in the MD simulations were calculated and whether the harmonic restraints on the zinc complex were used in an energy minimization prior to MD simulations.

To tackle this problem, new force field parameters for the zinc ion were laboriously developed within the AMBER force field paradigm by complying the reported procedures (Aqvist, 1990; Stote & Karplus, 1995). Unfortunately, with such parameters and even with the parameters developed within the CHARMM force field paradigm (Stote & Karplus, 1995), the four-ligand coordination in FT still could not be maintained in the MD simulations

performed with zinc coordinates in the protonation states described above.

These results eventually focused our attention on the protonation state of imidazole as a zinc ligand in proteins and prompted us to perform large basis set DFT calculations of the proton dissociation energy of zinc-coordinated imidazole. Our DFT calculations suggest that, like thiolate (Ryde, 1996) and the deprotonated peptide nitrogen atom (Rabenstein et al., 1985), the imidazole ring exists as imidazolate when coordinating to Zn^{2+} in proteins (ElYazal & Pang, 1999). Furthermore, our DFT calculations revealed that the imidazole-acetate dyad (Fig. 2) was converged to the imidazolate-acetic acid dyad (Fig. 2) in the presence of the hydroxide-coordinated zinc divalent cation after an energy minimization with the B3LYP/6-311+G(d,p) method. In the imidazole-acetate dyad, the nitrogen proton of the imidazole forms a hydrogen bond with the carboxylate oxygen atom, whereas in the imidazolate-acetic acid dyad, the oxygen proton of the acetic acid forms a hydrogen bond with the nitrogen atom of the imidazolate. In contrast, the imidazolate-acetic acid dyad was converged to the imidazole-acetate dyad in the absence of zinc after an energy minimization with the same method. These results suggest that the carboxylate group of Asp(Glu) in the second coordination shell of zinc in proteins serves as an effective proton acceptor for the zinc-coordinated imidazole proton donor. Accordingly, by using deprotonated, anionic $His^{-}363\beta$, $Cys^{-}299\beta$, $Asp^{-}297\beta$, and $HO^{-}1002$ in the first coordination shell, neutral $AspH359\beta$ in the second coordination shell, and a set of newly developed zinc parameters (r = 3.0 Å, ϵ = 1E−6 kcal/mol), the four-ligand coordination in FT was maintained in a 200 ps MD simulation. Unexpectedly, the four-ligand coordination was again converted to a five-ligand coordination when the simulation was extended to 500 ps. Even by using neutral $Asp352\beta$, the four-ligand coordination was still converted to the five-ligand coordination in a 650 ps MD simulation.

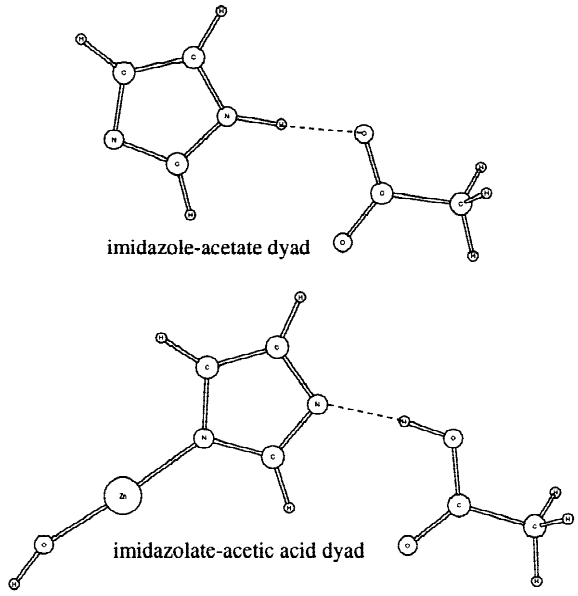

Fig. 2. Interchanges between the imidazole-acetate dyad and the imidazolate-acetic acid dyad influenced by the hydroxide-coordinated zinc divalent cation.

New method for simulating zinc proteins

The above results raised two fundamental questions: (1) Does Zn^{2+}, as a d^{10} closed shell divalent cation, really allow different coordination patterns (Purcell & Kotz, 1977)? (2) Are the nonbonded zinc parameters developed from a six-coordinate model in water applicable to simulations of a four-coordinate model in proteins? To answer these questions, we surveyed the zinc protein crystal structures deposited in the 1998 release of the Protein Data Bank (PDB) (Bernstein et al., 1977) and found that, among 114 zinc coordination complexes in 62 zinc proteins with resolutions better than 2.25 Å, the percentage of the five- and six-ligand zinc coordination complexes in proteins were only 26% (Roe & Pang, 1999). Furthermore, we discovered the inherent uncertainty in classifying zinc's five- and six-coordination patterns due to experimental resolution (Roe & Pang, 1999). We therefore proposed that the zinc divalent cation coordinates to only four ligands, because, in terms of energetics, its electronic structure favorably accommodates four pairs of electrons in its vacant $4s4p^3$ orbitals (Roe & Pang, 1999). Experimental observations of five- and six-ligand complexes were due to one or two pairs of ambidentate ligands that exchanged over time and were averaged as bidentate ligands (Roe & Pang, 1999).

The exclusive tetrahedral coordination concept immediately led us to devise a new method (Pang, 1999), named the "cationic dummy atom" method, for simulating zinc proteins. This method uses four identical cationic dummy atoms to mimic zinc's $4s4p^3$ vacant orbitals that accommodate the lone-pair electrons of zinc coordinates, thus imposing the requisite orientational requirement for zinc coordinates and simulating zinc's propensity for four-ligand coordination. The advantage of this method is the ability to maintain zinc's four-ligand coordination in proteins during nanosecond-length MD simulations without use of harmonic restraints that rigidify the zinc-containing active site. It, hence, permits evaluation of the binding free energy of zinc ligands and simulation of the exchanges of zinc's ambidentate coordinates in proteins (Pang, 1999). Furthermore, unlike the force field parameters developed using the bonded model with either harmonic potential or anharmonic potential, the force field parameters developed using the cationic dummy atom method are usable in docking studies of zinc proteins (Perola et al., 2000). Conceptually, the "cationic dummy atom method" is different from the "seven-electrostatic-center approach" proposed for modeling zinc proteins (Aqvist & Warshel, 1990, 1992). The former uses four cationic dummy atoms with explicit mass to mimic zinc's $4s4p^3$ vacant orbitals and is able to simulate zinc's propensity for four-ligand coordination in proteins (Pang, 1999). The latter uses six peripheral, fractional positive charges to improve the calculated solvation energies of transition-metal ions and failed to simulate zinc's propensity for four-ligand coordination in proteins (Aqvist & Warshel, 1990, 1992). The cationic dummy atom method comprises three steps: (1) building a five-atom zinc divalent cation, termed "tetrahedral zinc divalent cation," having a center atom and four identical dummy atoms located at the apices of a tetrahedron; (2) assigning van der Waals parameters (r = 3.1 Å, ϵ = 1E−6 kcal/mol), zero charge, and a mass of 65.380 to the center atom; and (3) assigning "+0.5" charge, zero r and e, and a mass of 0.1 to the four dummy atoms that are covalently bonded to the center atom with the parameters listed in Table 1 (Pang, 1999).

Table 1. *Additional force field parameters for zinc protein simulations [for definitions of the atom names see reference (Cornell et al., 1995)]*

Force field parameters of the tetrahedral zinc ion

Bond	K [kcal/(mol Å^2)]	R_{eq} (Å)
DZ-ZN	540.0	0.90

Angle	K [kcal/(mol radian^2)]	T_{eq} (deg)
DZ-ZN-DZ	55.0	109.50
DZ-DZ-DZ	55.0	60.0
DZ-DZ-ZN	55.0	35.25

RESP charges of histidinate

Atom name	Charge	Atom name	Charge
N	−0.5641	ND1	−0.7626
H	0.2469	CE1	0.4994
CA	0.3171	HE1	−0.0295
HA	0.0096	NE2	−0.7656
CB	−0.1347	CD2	0.0405
HB2	0.0083	HD2	0.0525
HB3	0.0381	C	0.4588
CG	0.1504	O	−0.5653

RESP charges of hydroxide

Atom name	Charge	Atom name	Charge
HO	0.2049	OH	−1.2049

Table 2. *RMSD between the X-ray structure (PDB code: 1FT1) and the structures (excluding H, Na^+, and Cl^- atoms) averaged over 0.5 and 1.0 ns MD simulations, respectively (zinc complex: Zn^{2+}, $Cys^-299\beta$, $His^-363\beta$, $Asp^-297\beta$, and HO^-1002; active site: see Table 4 for the definition)*

	RMSD [Å (No. of matched atoms)]		
Average structure	Zinc complex	Active site	Protein
0.5 ns	0.70 (30)	0.89 (454)	1.16 (4028)
1.0 ns	0.68 (30)	1.04 (454)	1.19 (4028)

Conservation of the tetrahedral zinc complex

By using the tetrahedral zinc divalent cation, four anionic first-shell ligands (His363β, Cys299β, Asp297β, and HO1002), and one neutral second-shell ligand (AspH359β), the four-ligand coordination of zinc in FT was able to be simulated for 1.0 ns (1.0 fs time step). In another MD simulation of FT complexed with farnesyl pyrophosphate, the tetrahedral zinc complex was maintained for 2.0 ns (1.0 fs time step) (K. Yu, Y.-P. Pang, & F.G. Prendergast, in prep.). The root-mean-square deviations (RMSDs) of the four-ligand zinc complex in FT between the X-ray structure (PDB code: 1FT1) and the time-average structures of the 0.5 and 1.0 ns MD simulations are 0.70 and 0.68 Å, respectively (Table 2), indicating that the two MD simulations were equilibrated and the four-ligand coordination was well kept throughout the MD simulations.

As depicted in Figure 3, the zinc interatomic distances fluctuate around the values calculated from two X-ray structures of FT (Table 3) (Park et al., 1997; Dunten et al., 1998). The average zinc interatomic distances and the average angles of the zinc coordinates were in agreement, within experimental error, with the corresponding values obtained from the X-ray structures (Table 3). Asp352β, that hitherto always moved toward the zinc ion in the MD simulations without use of the cationic dummy atom method, stayed in the desired position during the entire 1.0 ns MD simulation employing the cationic dummy atom method (Fig. 3). This is because the cationic dummy atom method is able to distribute the charge of the zinc divalent cation to its coordinates making the zinc divalent cation not attractive to the anionic Asp352β. Furthermore, the FT structure bound with the tetrahedral zinc divalent cation did not diverge from the X-ray structures during the 1.0 ns MD simulation. This is evident from the RMSDs of all the non-hydrogen atoms between the X-ray structure and the average structure of the 1.0 ns MD simulation (Table 2). It is also evident from the interatomic distances of some residues in the active site in comparison with the values obtained from the X-ray structures (Table 3). The averaged interatomic distances between Zn^{2+} and the two carboxylate oxygen atoms of Asp352β (Zn^{2+}-OD1 and Zn^{2+}-OD2) are in excellent agreement with those obtained from the X-ray structures (Table 3). Interestingly, the corresponding distances in the instantaneous structures collected at 1.0 ps intervals during the 1.0 ns MD simulation (Fig. 3) reveal exchanges of the two oxygen atoms of the carboxylate group of Asp352β, which is not identifiable from the X-ray structure.

Active site conformational flexibility

From visual inspection of the X-ray structure of FT, 50 residues listed in Table 4 can be defined as active-site residues. The mean deviations of $\chi 1$ and $\chi 2$ of the 50 residues in all the instantaneous structures obtained at 1.0 ps intervals during the 1.0 ns MD simulation are depicted Figure 4. The mean deviation is defined as $\sqrt{[\sum x^2 - (\sum x)^2/n]/(n-1)}$. The $\chi 1$ and $\chi 2$ are defined as C-CA-CB-CG and CA-CB-CG-X, respectively; the atom name are defined in reference (Cornell et al., 1995). As indicated in the $\chi 1$ and $\chi 2$ mean deviation plots (Fig. 4), 41 active-site residues were relatively immobile during the 1.0 ns MD simulation. The RMSDs of the 50 active site residues and the backbone atoms of the these residues between the average MD and X-ray structures are 1.04 and 0.68 Å (Table 2), respectively, indicating that no large conformational change occurred in the active site during the MD simulation.

Use of 15° of arc as a cutoff, the $\chi 1$ mean deviation plot reveals that six residues (Gln162α, Gln195α, Lys294β, Leu295b, Lys353β, and Ser357β) in the active site are relatively mobile. Use of a higher cutoff at 30° of arc, the $\chi 2$ mean deviation plot reveals that eight residues (Asn127α, Gln162α, Asn165α, Asp196α, His248β, Lys294β, Leu295β, and Asp352β) are mobile. A further examination of the plots of $\chi 2$ vs. time reveal that $\chi 2$ of the two Asp residues vary with increments of ~180° of arc, indicating intramolecular exchange of the two carboxy oxygen atoms of the two

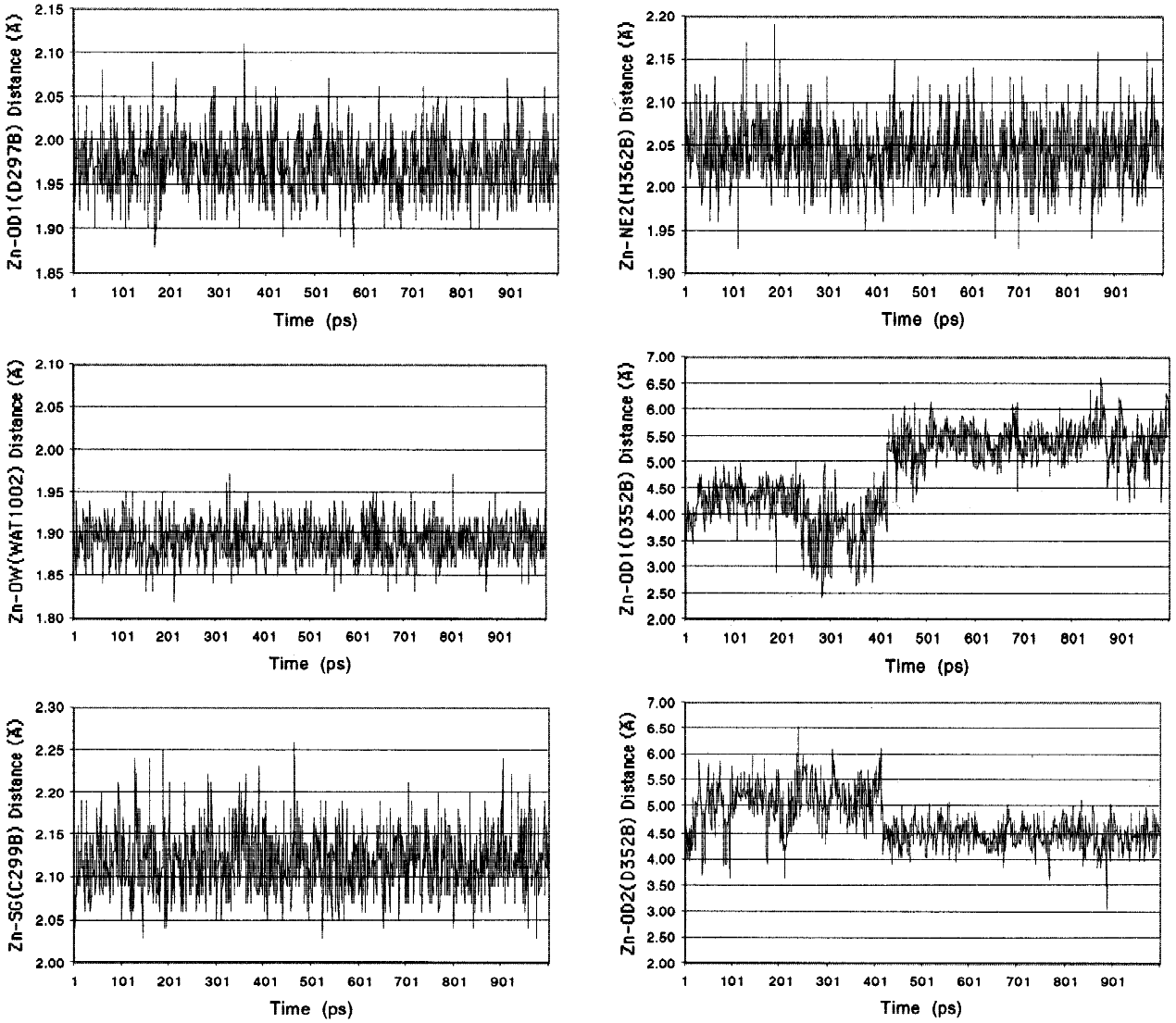

Fig. 3. Interatomic distances calculated from the instantaneous structures obtained at 1.0 ps intervals during the 1.0 ns MD simulation.

Asp residues during the simulation. Nevertheless, the exchanges of the two carboxy oxygen atoms are beyond our interest, since this motion is equivalent to the rotation of a methyl group of Ala that does not critically contribute to the conformational flexibility of the active site relevant to drug screen and design. Combining the non-Asp, mobile residues identified from $\chi 1$ and $\chi 2$ plots, it is conceivable that nine residues (Asn127α, Gln162α, Asn165α, Gln195α, His248β, Lys294β, Leu295β, Lys353β, and Ser357β) in the active site are relatively mobile in the MD simulation in water.

Data deposition

The coordinates of the average structure of the substrate-free, zinc-bound FT derived from the 1.0 ns MD simulation was deposited to the PDB (Bernstein et al., 1977) on July 12, 1999 (PDB code: 1QE2). The coordinates of the corresponding instantaneous structures are available upon request.

Discussion

One potential concern about the successful MD simulation of FT described here is the use of the anionic first-shell zinc ligands in FT. On one hand, limited by the current experimental resolution of X-ray crystallography and NMR spectroscopy and of other amenable spectroscopic techniques, it is uncertain if all the first-shell coordinates are deprotonated in FT. However, *it is also uncertain whether all the first-shell ligands are not deprotonated.* On the other hand, it has long been assumed that all four cysteine coordinates are deprotonated in the zinc complex of alcohol dehydrogenase (Eklund & Branden, 1983; Pettersson, 1987; Ryde, 1996). On the basis of the *interpretation* of the electronic spectra of a cobalt-substituted enzyme, only two deprotonated cysteine residues in the zinc complex of alcohol dehydrogenase have also been hypothesized (Garmer & Krauss, 1993). However, this hypothesis is questionable since zinc is a d^{10} closed shell divalent cation, whereas Co^{2+} is a d^7 open shell divalent cation (Roe & Pang,

Table 3. *Interatomic distances (Å) and angles (degree of arc) of the zinc coordination ligands calculated from the structures of the 1.0 ns MD simulations and the X-ray structures (I: the zinc-bound FT, 1ft1, resolution at 2.25 Å; and II: the zinc and co-substrate-bound FT, 1fpp, resolution at 2.75 Å)*[a]

	Average ± deviation (no.)		
	MD structure	X-ray structure I	X-ray structure II
Zn-OW (Wat^{1002})	1.9 ± 0.02 (1,000)	2.7 ± 0.8 (1)	3.2 ± 0.8 (1)
Zn-OD1 ($D^{297\beta}$)	2.0 ± 0.03 (1,000)	2.0 ± 0.8 (1)	2.0 ± 0.7 (1)
Zn-NE2 ($H^{363\beta}$)	2.0 ± 0.04 (1,000)	2.5 ± 0.8 (1)	2.1 ± 0.7 (1)
Zn-SG ($C^{299\beta}$)	2.1 ± 0.04 (1,000)	2.2 ± 0.8 (1)	2.3 ± 0.7 (1)
Zn-OD2 ($D^{297\beta}$)	3.6 ± 0.2 (1,000)	2.6 ± 0.8 (1)	2.0 ± 0.8 (1)
Zn-CG ($D^{297\beta}$)	3.1 ± 0.7 (1,000)	2.6 ± 0.8 (1)	2.3 ± 0.7 (1)
Zn-CB ($C^{299\beta}$)	3.6 ± 0.1 (1,000)	3.5 ± 0.8 (1)	3.4 ± 0.7 (1)
Zn-ND1 ($H^{363\beta}$)	4.1 ± 0.1 (1,000)	4.5 ± 0.8 (1)	4.1 ± 0.7 (1)
Zn-OD1 ($D^{359\beta}$)	7.0 ± 0.2 (1,000)	7.0 ± 0.7 (1)	7.2 ± 0.8 (1)
Zn-OD2 ($D^{359\beta}$)	6.7 ± 0.2 (1,000)	7.3 ± 0.7 (1)	6.7 ± 0.8 (1)
Zn-CG ($D^{359\beta}$)	7.4 ± 0.1 (1,000)	7.6 ± 0.8 (1)	7.4 ± 0.7 (1)
Zn-OD1 ($D^{352\beta}$)	4.8 ± 0.8 (1,000)	5.0 ± 0.8 (1)	4.9 ± 0.8 (1)
Zn-OD2 ($D^{352\beta}$)	4.7 ± 0.5 (1,000)	4.8 ± 0.8 (1)	4.4 ± 0.8 (1)
Zn-CG ($D^{352\beta}$)	4.7 ± 0.3 (1,000)	4.6 ± 0.8 (1)	4.4 ± 0.8 (1)
Zn-NZ ($D^{353\beta}$)	6.4 ± 0.4 (1,000)	8.2 ± 0.8 (1)	7.1 ± 0.7 (1)
Zn-CE ($D^{353\beta}$)	7.7 ± 0.4 (1,000)	7.6 ± 0.8 (1)	8.6 ± 0.7 (1)
Zn-OH ($Y^{300\beta}$)	5.7 ± 0.4 (1,000)	5.7 ± 0.9 (1)	6.0 ± 0.8 (1)
Zn-CZ ($R^{202\beta}$)	11.3 ± 0.4 (1,000)	11.9 ± 1.0 (1)	14.6 ± 0.9 (1)
Zn-OH ($Y^{166\alpha}$)	19.6 ± 0.4 (1,000)	20.1 ± 0.9 (1)	19.5 ± 1.0 (1)
Zn-ND1 ($H^{201\alpha}$)	14.8 ± 0.6 (1,000)	14.5 ± 0.9 (1)	14.8 ± 0.7 (1)
Zn-CZ ($R^{291\beta}$)	11.8 ± 0.4 (1,000)	11.7 ± 0.8 (1)	11.8 ± 0.7 (1)
Zn-OH ($Y^{361\beta}$)	5.3 ± 0.7 (1,000)	4.6 ± 0.8 (1)	4.6 ± 0.7 (1)
$OD1^{297\beta}$-Zn-OW^{1002}	110 ± 4 (1,000)	98 ± 5 (1)	85 ± 5 (1)
$OD1^{297\beta}$-Zn-$SG^{299\beta}$	105 ± 4 (1,000)	104 ± 5 (1)	109 ± 5 (1)
$OD1^{297\beta}$-Zn-$NE2^{363\beta}$	112 ± 5 (1,000)	120 ± 5 (1)	132 ± 5 (1)
OW^{1002}-Zn-$SG^{299\beta}$	110 ± 3 (1,000)	119 ± 5 (1)	105 ± 5 (1)
OW^{1002}-Zn-$NE2^{363\beta}$	109 ± 4 (1,000)	97 ± 5 (1)	110 ± 5 (1)
$SG^{299\beta}$-Zn-$NE2^{363\beta}$	110 ± 4 (1,000)	118 ± 5 (1)	110 ± 5 (1)

[a]The deviation of the distance in the X-ray structure was estimated from $\sqrt{(B_i + B_j)/(8\pi^2)}$, where B_i and B_j are the B values of atoms i and j, respectively. The angle deviation in the X-ray structure was estimated from ATAN($\Delta D/D$), where DD is the average deviation of the X-Zn distance (0.2 Å) and D is the average distance of X-Zn (2.2 Å), and X represents N, O, and S atoms.

1999). Indeed, ab initio calculations of zinc coordination models in alcohol dehydrogenase reported thereafter have confirmed that all the four cysteines are deprotonated in the zinc complex of alcohol dehydrogenase (Ryde, 1996). Therefore, it is reasonable to use four deprotonated anionic zinc ligands in the MD simulation of FT.

In the present study, the FT structure was simulated using the cationic dummy atom approach with: (1) HO^-, Asp^-, HisH, and CysH in the first coordination-shell and Asp^- in the second-coordination shell; (2) HO^-, Asp^-, HisH, and Cys^- in the first coordination-shell and Asp^- in the second coordination-shell; (3) H_2O, Asp^-, HisH, and Cys^- in the first coordination-shell and Asp^- in the second coordination-shell; and (4) HO^-, Asp^-, His^-, and Cys^- in the first coordination-shell and AspH in the second coordination-shell. Only the MD simulation with four anionic first-shell coordinates yielded an average structure nearly identical to the X-ray structures of FT (Tables 2, 3). This justifies the use of four anionic coordinates in the MD simulation of FT a posteriori as MD simulation itself is an empirical approach. Additional justification for the use of four anionic coordinates in the MD simulation of FT is the results from our reported 2.0 ns MD simulations of carbonic anhydrase (PDB code: 1CA2), carboxypeptidase A (PDB code: 5CPA), and rubredoxin (PDB code: 1IRN) employing the cationic dummy atom approach (Pang, 1999). In these MD simulations, only the use of four anionic coordinates resulted in average structures nearly identical to the corresponding crystal structures (Pang, 1999).

Analysis of the FT sequences in various species retrieved from Entrez at the NCBI (Entrez, 1999) revealed that the nine mobile residues identified by the MD simulation are conserved in mammals according to the sequence alignment carried out by the SIM program provided at ExPASy (ExPASy, 1999). This result indicates that our conformational analysis is biologically relevant. Some of the nine mobile residues might be involved in ligand-induced active site conformational rearrangement upon binding. Indeed, in the X-ray structure of the FPP-bound FT, His248β and Lys294β directly interact with the two phosphate groups of the co-substrate farnesyl pyrophosphate. In the "free" FT crystal structure (PDB code: 1FT1) (Park et al., 1997), Ser357β is in contact with the carboxy-terminal residues of a symmetry-related FT.

The present work offers evidence that the "cationic dummy atom method" can effectively solve the problem of deformation of the tetrahedral zinc complex that commonly seen in conventional MD simulations of zinc proteins. A successful 1.0 ns (1.0 fs time step) MD simulation of zinc-bound FT suggests that, for screening

Table 4. *Active site residues and their IDs used in conformational flexibility analysis*

Id	Name	Id	Name	Id	Name
1	Asn127α	18	Leu96β	35	Cys254β
2	Ala129α	19	Ser99β	36	Arg291β
3	Gln162α	20	Trp102β	37	Lys294β
4	Lys164α	21	Trp106β	38	Leu295β
5	Asn165α	22	His149β	39	Asp297β
6	Tyr166α	23	Ala151β	40	Cys299β
7	Gln167α	24	Tyr154β	41	Tyr300β
8	Gln195α	25	Met193β	42	Trp303β
9	Asp196α	26	Asp200β	43	Asp352β
10	Lys198α	27	Arg202β	44	Lys353β
11	Asn199α	28	Ser203β	45	Lys356β
12	Tyr200α	29	Tyr205β	46	Ser357β
13	His201α	30	Cys206β	47	Asp359β
14	Val43β	31	His248β	48	Tyr361β
15	Glu47β	32	Gly249β	49	His363β
16	Tyr93β	33	Gly250β	50	Tyr365β
17	Cys95β	34	Tyr251β		

and design of new FTIs that interact with the relatively immobile residues in the active site observed in the MD simulation, both the X-ray structure of FT and the FT structures derived from the MD simulation can be usable as drug targets. To screen and design inhibitors that interact with the mobile residues in the active site identified by the MD simulation, use of the X-ray structure alone might not be sufficient. Alternative side-chain conformations of the mobile residues could be useful in screening and design, especially in FT structure-based design of farnesyl pyrophosphate analogs as FTI (Leonard, 1997), since His248β and Lys294β interact with farnesyl pyrophosphate in the crystal structure of farnesyl pyrophosphate-bound FT (Long et al., 1998).

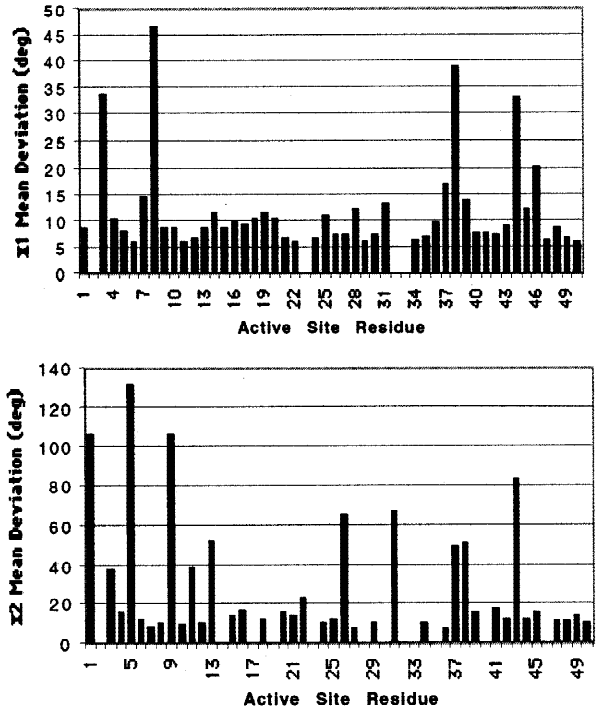

Fig. 4. Mean deviations of $\chi 1$ and $\chi 2$ values of the 50 active site residues in the 1,000 instantaneous structures collected at 1.0 ps intervals during the 1.0 ns MD simulation.

Materials and methods

FT structure

The initial structure of FT used in our MD simulations was taken and modified from the X-ray structure of rat FT (PDB code: 1FT1) (Park et al., 1997). The modification procedure included: (1) addition of hydrogen atoms; (2) protonation or deprotonation of the Arg, Lys, Asp, Glu, His, and Cys residues; (3) addition of counter ions to neutralize the charged residues; and (4) energy minimizations of the introduced hydrogen atoms and counter ions of the system. To determine the protonation state, all the Arg, Lys, Asp, Glu, His, and Cys residues were visually inspected. Asp and Glu were treated as deprotonated, otherwise as protonated if they were located in a hydrophobic environment or in the second coordination shell of zinc. One Na^+ cation was placed in the vicinity of a deprotonated, anionic residue if this residue was more than 8 Å away from a cationic residue. Arg and Lys were treated as protonated unless they were surrounded by hydrophobic residues. One Cl^- anion was introduced next to the protonated, cationic residue if this residue was more than 8 Å away from an anionic residue. His was treated as deprotonated, anionic histidinate when coordinating to zinc (ElYazal & Pang, 1999). His, not coordinating to zinc, was treated as protonated if it was $<$8 Å away from an acidic residue, otherwise it was treated as neutral. In the structure of the neutral His, one proton was attached to the delta nitrogen atom of the imidazole ring if the resulting tautomer formed more hydrogen bonds in the protein; otherwise the proton was attached to the epsilon nitrogen atom. Cys was treated as deprotonated when coordinating to zinc (Ryde, 1996). The location of every counter ion was determined by energy minimization with a positional constraint applied to all atoms of the system except for the counter ion. Such energy minimizations were performed with a nonbonded cutoff of 8.0 Å and a dielectric constant of 1.0.

The terminal residues of the two subunits were excised since they were away from the active site to reduce the size of the protein so that a nanosecond-length MD simulation could be performed on a dedicated SGI Origin 2000 supercomputer (8xR10,000, 195Mhz). In the truncated FT structure (α subunit: residues 116–247, β subunit: residues 41–406), all the Glu and Asp residues were deprotonated except that Asp359β was treated as neutral. All the Arg and Lys residues were protonated. Cys299β was deprotonated. His109β and His375β were protonated. His135α, His171α, His201α, His205α, His241α, His66β, His78β, His80β, His149β, His248β, His312β, His316β, His331β, and His398β were assigned as the HIE (N^{ϵ}-H) tautomer, while His170α, His194β, His327β, and His383β were assigned as the HID (N^{δ}-H) tautomer. His363β and H_2O1002 were treated as histidinate and hydroxide, respectively. Asp122α, Asp181α, Asp191α, Asp217α, Asp91β, Asp220β, Glu160α, Glu161α, Glu187α, Glu52β, Glu57β, Glu94β, Glu131β, Glu166β, Glu167β, Glu391β, Arg138α, Arg142α,

Arg70β, Arg84β, Arg266β, and Arg358β were each neutralized by adding a counter ion (Na^+ or Cl^-), respectively, so that the total charge of the system was zero.

MD simulation

All the MD simulations were performed by employing the AMBER 5.0 program (Pearlman et al., 1995) with the Cornell et al. (1995) force field and additional force field parameters listed in Table 1 for simulating zinc proteins without use of covalent bonds or harmonic restraints to maintain the tetrahedral zinc complex in proteins (Pang, 1999). The values of the keywords in upper-case letters used by the AMBER program are described in parentheses. All the MD simulations used: (1) the SHAKE procedure for all bonds of the system (NTC = 3 and NTF = 3) (Ryckaert et al., 1977); (2) a time step of 1.0 fs (DT = 0.001); (3) a dielectric constant e = 1.0 (IDIEL = 1.0); (4) the Berendsen coupling algorithm (NTT = 1) (Berendsen et al., 1984); (5) the Particle Mesh Ewald method (Darden et al., 1993) used to calculate the electrostatic interactions (BOXX = 91.4869, BOXY = 77.6960, BOXZ = 69.3721, ALPHA = BETA = GAMMA = 90.0, NFFTX = 81, NFFTY = 81, NFFTZ = 64, SPLINE_ORDER = 4, ISCHARGED = 0, EXACT_EWALD = 0, DSUM_TOL = 0.00001); (6) the nonbonded atom pair list updated at every 20 steps (NSNB = 20); (7) a distance cutoff of 8.0 Å used to calculate the nonbonded steric interactions (CUT = 8.0); and (8) default values of all other keywords not mentioned here. The truncated FT structure was simulated in a TIP3P (Jorgensen et al., 1982) water box with a periodic boundary condition at constant temperature and pressure (NCUBE = 20, QH = 0.4170, DISO = 2.20, DISH = 2.00, CUTX = CUTY = CUTZ = 8.2, NTB = 2, TEMP0 = 298, PRES0 = 1, TAUTP = 0.2, TAUTS = 0.2, TAUP = 0.2, NPSCAL = 0, and NTP = 1). The resulting system consisting of 45,286 atoms was first energy minimized for 500 steps to remove close van der Waals contacts in the system. The minimized system was then slowly heated to 298 K (10K/ps, NTX = 1) and equilibrated for 50 ps before simulation.

Density functional theory calculations

The density functional theory (DFT) calculations were carried out by using the Gaussian 98 program revision A.7 (Frisch et al., 1999) running on an SGI Origin 2000 (8 × R10,000, 195 Mhz, 2.0 GB memory, and 40 GB disk). The imidazole-carboxylate dyad structures in the presence and absence of the hydroxide-coordinated zinc divalent cation (Fig. 2) were generated with the Quanta program and optimized by an energy minimization with the CHARMm molecular mechanics force field (QUANTA/CHARMm). Further geometry optimizations and harmonic frequencies used to identify minimal energy geometries were computed by using Becke's three-parameter formulation (B3LYP) density functional method (Lee et al., 1988; Becke, 1993) with the 6-311+G(d,p) basis set. This basis set has been reported to be successful in computing the hydration energy of the zinc divalent cation (Hehre et al., 1986; Pavlov et al., 1998).

Note added in proof

The masses of the dummy atom (DZ) and the zinc atom (ZN) should be changed to 1.0 and 61.38, respectively, if the cationic dummy atom approach is used in the MD simulations without SHAKE (NTC = 1) or with SHAKE applied to bonds involving hydrogen atom (NTC = 2).

Acknowledgments

This work was supported by the Mayo Foundation for Medical Education and Research. K. Xu's training has been supported, in part, by a NIH training grant (CA 75926) to the Tumor Biology Program of the Mayo Graduate School and by the Mayo Clinic and Foundation.

References

Aqvist J. 1990. Ion-water interaction potentials derived from free energy perturbation simulations. *J Phys Chem 94*:8021–8224.

Aqvist J, Warshel A. 1990. Free energy relationships in metalloenzyme-catalyzed reactions. Calculations of the effects of metal ion substitutions in staphylococcal nuclease. *J Am Chem Soc 112*:2860–2868.

Aqvist J, Warshel A. 1992. Computer simulation of the initial proton transfer step in human carbonic anhydrase I. *J Mol Biol 224*:7–14.

Becke AD. 1993. Density-functional thermochemistry. 3. The role of exact exchange. *J Chem Phys 98*:5648–5652.

Berendsen HJC, Postma JPM, van Gunsteren WF, Di Nola A, Haak JR. 1984. Molecular dynamics with coupling to an external bath. *J Chem Phys 81*: 3684–3690.

Bernstein FC, Koetzle TF, Williams GJ, Meyer EE Jr, Brice MD, Rodgers JR, Kennard O, Shimanouchi T, Tasumi M. 1977. The Protein Data Bank: A computer-based archival file for macromolecular structures. *J Mol Biol 112*:535–542.

Cornell WD, Cieplak P, Bayly CI, Gould IR, Merz KM Jr, Ferguson DM, Spellmeyer DC, Fox T, Caldwell JW, Kollman PA. 1995. A second generation force field for the simulation of proteins, nucleic acids, and organic molecules. *J Am Chem Soc 117*:5179–5197.

Darden TA, York D, Pedersen L. 1993. Particle Mesh Ewald: An N log(N) method for Ewald sums in large systems. *J Chem Phys 98*:10089.

Dunten P, Kammlott U, Crowther R, Weber D, Palermo R, Birktoft J. 1998. Protein farnesyltransferase—Structure and implications for substrate binding. *Biochemistry 37*:7907–7912.

Eklund H, Branden C-T. 1983. The role of zinc in alcohol dehydrogenase. In: Spiro TG, ed. *Zinc enzymes*. New York: John Wiley & Sons. pp 124–153.

ElYazal J, Pang YP. 1999. *Ab initio* calculations of proton dissociation energies of zinc ligands: Hypothesis of imidazolate as zinc ligand in proteins. *J Phys Chem B 103*:8773–8779.

Entrez. 1999. http://www.ncbi.nlm.nih.gov.

ExPASy. 1999. http://www.expasy.ch/sprot.

Frisch MJ, Trucks GW, Schlegel HB, Gill PMW, Hohnson BG, Robb MA, Raghavachari K, Al-Laham MA, Zakrzewski VG, Ortiz JV, et al. 1999. GAUSSIAN 98, Revision A.7. Pittsburgh, Pennsylvania: Gaussian, Inc.

Garmer DR, Krauss M. 1993. Ab initio quantum chemical study of the cobalt d-d spectroscopy of several substituted zinc enzyme. *J Am Chem Soc 115*:10247–10257.

Gibbs JB, Oliff A. 1997. The potential of farnesyltransferase inhibitors as cancer chemotherapeutics. *Annu Rev Pharmacol Toxicol 37*:143–166.

Hehre WJ, Radom L, Schleyer PVR, Pople J. 1986. *Ab initio molecular orbital theory*. New York: Wiley. pp 82–83.

Hoops SC, Anderson KW, Merz KMJ. 1991. Force field design for metalloproteins. *J Am Chem Soc 113*:8262–8270.

Jorgensen WL, Chandreskhar J, Madura JD, Impey RW, Klein ML. 1982. Comparison of simple potential functions for simulating liquid water. *J Chem Phys 79*:926–935.

Kohl NE, Mosser SD, deSolms SJ, Giuliani EA, Pompliano DL, Graham SL, Smith RL, Scolnick EM, Oliff A, Gibbs JB. 1993. Selective inhibition of ras-dependent transformation by a farnesyltransferase inhibitor. *Science 260*:1934–1937.

Lee C, Yang W, Parr RG. 1988. Development of the Colle-Salvetti correlation-energy formula into a functional of the electron density. *Phys Rev B37*:785.

Leonard DM. 1997. Ras farnesyltransferase: A new therapeutic target. *J Med Chem 40*:2971–2990.

Long SB, Casey PJ, Beese LS. 1998. Cocrystal structure of protein farnesyltransferase complexed with a farnesyl diphosphate substrate. *Biochemistry 37*:9612–9618.

Long SB, Casey PJ, Beese LS. 2000. The basis for K-Ras4B binding specificity to protein farnesyl-transferase revealed by 2 angstrom resolution ternary complex structures. *Struct Fold Des 8*:209–222.

Lu DS, Voth GA. 1998. Molecular dynamics simulations of human carbonic anhydrase II: Insight into experimental results and the role of solvation. *Proteins 33*:119–134.

Pang YP. 1999. Novel zinc protein molecular dynamics simulations: Steps toward antiangiogenesis for cancer treatment. *J Mol Model 5*:196–202.

Park HW, Boduluri SR, Moomaw JF, Casey PJ, Beese LS. 1997. Crystal structure of protein farnesyltransferase at 2.25 angstrom resolution. *Science 275*:1800–1804.

Pavlov M, Siegbahn PEM, Sandstrom M. 1998. Hydration of beryllium, magnesium, calcium, and zinc ions using density functional theory. *J Phys Chem 102*:219–228.

Pearlman DA, Case DA, Caldwell JW, Ross WS, Cheatham TE III, Debolt S, Ferguson D, Seibel G, Kollman PA. 1995. AMBER, a package of computer programs for applying molecular mechanics, normal mode analysis, molecular dynamics and free energy calculations to simulate the structural and energetic properties of molecules. *Comput Phys Commun 91*:1–41.

Perola E, Xu K, Kollmeyer TM, Kaufmann SH, Prendergast FG, Pang YP. 2000. Successful virtual screening of a chemical database for farnesyltransferase inhibitor leads. *J Med Chem 43*:401–408.

Pettersson G. 1987. Liver alcohol dehydrogenase. *CRC Crit Rev Biochem 21*:349–389.

Prendergast GC, Davide JP, deSolms SJ, Giuliani EA, Graham SL, Gibbs JB, Oliff A, Kohl NE. 1994. Farnesyltransferase inhibition causes morphological reversion of ras-transformed cells by a complex mechanism that involves regulation of the actin cytoskeleton. *Mol Cell Biol 14*:4193–4202.

Purcell KF, Kotz JC. 1977. *Inorganic chemistry*. Philadelphia: Saunders, WB. pp 1215–1217.

QUANTA/CHARMm. 1997. San Diego, California: Molecular Simulations Inc.

Rabenstein DL, Daignault SA, Isab AA, Arnold AP, Shoukry MM. 1985. Nuclear magnetic resonance studies of the solution chemistry of metal complexes. 21. The complexation of zinc by glycylhistidine and alanylhistidine peptides. *J Am Chem Soc 107*:6436–6439.

Reiss Y, Goldstein JL, Seabra MC, Casey PJ, Brown MS. 1990. Inhibition of purified p21ras farnesyl: Protein transferase by Cys-AAX tetrapeptides. *Cell 62*:81–88.

Roe RR, Pang YP. 1999. Zinc's exclusive tetrahedral coordination governed by its electronic structure. *J Mol Model 5*:134–140.

Ryckaert JP, Ciccotti G, Berendsen HJC. 1977. Numerical integration of the Cartesian equations of motion of a system with constraints: Molecular dynamics of n-alkanes. *J Comput Phys 23*:327–341.

Ryde U. 1995. Molecular dynamics simulations of alcohol dehydrogenase with a four- or five-coordinate catalytic zinc ion. *Proteins 21*:40–56.

Ryde U. 1996. The coordination chemistry of the structural zinc ion in alcohol dehydrogenase studied by ab initio quantum chemical calculations. *Eur Biophys J 24*:213–221.

Sebti SM, Hamilton AD. 1997. Inhibition of Ras prenylation: A novel approach to cancer chemotherapy. *Pharmacol Ther 74*:103–114.

Stote RH, Karplus M. 1995. Zinc binding in proteins and solution: A simple but accurate nonbonded representation. *Proteins 23*:12–31.

Strickland CL, Weber PC, Windsor WT, Wu Z, Le HV, Albanese MM, Alvarez CS, Cesarz D, del Rosario J, Deskus J, et al. 1999. Tricyclic farnesyl protein transferase inhibitors: Crystallographic and calorimetric studies of structure-activity relationships. *J Med Chem 42*:2125–2135.

Strickland CL, Windsor WT, Syto R, Wang L, Bond R, Wu Z, Schwartz J, Le HV, Beese LS, Weber PC. 1998. Crystal structure of farnesyl protein transferase complexed with a CaaX peptide and farnesyl diphosphate analogue. *Biochemistry 37*:16601–16611.

Vedani A, Huhta DW. 1990. A new force field for modeling metalloproteins. *J Am Chem Soc 112*:4759–4767.

Wasserman ZR, Hodge CN. 1996. Fitting an inhibitor into the active site of thermolysin: A molecular dynamics case study. *Proteins 24*:227–237.

Wu Z, Demma M, Strickland CL, Syto R, Le HV, Windsor WT, Weber PC. 1999. High-level expression, purification, kinetic characterization and crystallization of protein farnesyltransferase beta-subunit C-terminal mutants. *Protein Eng 12*:341–348.